SUPPLEMENTARY MATERIAL

Dopaminergic medication normalizes aberrant cognitive control circuit signaling in Parkinson's disease

Weidong Cai[1,2], Christina B. Young[3], Rui Yuan[1], Byeongwook Lee[1], Sephira Ryman[3], Jeehyun Kim[3], Laurice Yang[3], Victor W. Henderson[2,3,4], Kathleen L. Poston[2,3,5], and Vinod Menon[1,2,3]

Supplementary Methods

Medication ON versus OFF order

To minimize the physical discomfort experienced by PD participants when are OFF dopaminergic medications, the OFF session was scheduled at a time based on patient convenience and preference; therefore, the ON versus OFF order was not fully counterbalanced across PD participants. The mean (SD) time between ON and OFF scans was 16 (109) days with 12 PD participants who had their OFF scan first and 24 PD participants who had their ON scan first. We confirmed that unbalanced ON vs. OFF order does not significantly affect any result reported in this study. See **Supplementary Results** below.

fMRI preprocessing

We used SPM12 software package (http://www.fil.ion.ucl.ac.uk/spm/software/spm12/), as well as in-house programs in MATLAB (MathWorks). Functional MRI data were first slice time corrected, aligned to the averaged time frame to correct for head motion, and co-registered with each participant's T1-weighted images. Structural MRI images were segmented into grey matter, white matter, and cerebrospinal fluid. Based on the transformation matrix from structural image, the functional images were then transformed to the standard Montreal Neurological Institute (MNI) template in 2x2x2 mm^3 by using the Diffeomorphic Anatomical Registration Through Exponentiated Lie algebra (DARTEL) toolbox [1]. A 6-mm Gaussian kernel was used to spatially smooth the functional images. Participants with more than 3mm head motion were excluded.

MDSI model for estimating causal interactions from fMRI data

MDSI estimates context-dependent causal interactions between multiple brain regions in latent quasi-neuronal state while accounting for variations in hemodynamic responses in these regions. MDSI has been validated using extensive simulations [22-24] and has been successfully applied to our previous studies [25-27]. MDSI models the multivariate fMRI time series by the following state-space equations:

$$\boldsymbol{s}(t) = \sum_{j=1}^{J} v_j(t) C_j \, \boldsymbol{s}(t-1) + \boldsymbol{w}(t) \quad (1)$$

$$\boldsymbol{x}_m(t) = [\boldsymbol{s}_m(t) \; \boldsymbol{s}_m(t-1) \; \ldots . \boldsymbol{s}_m(t-L+1)]' \quad (2)$$

$$y_m(t) = b_m \Phi \boldsymbol{x}_m(t) + \boldsymbol{e}_m(t) \quad (3)$$

In Equation (1), $\boldsymbol{s}(t)$ is a $M \times 1$ vector of latent quasi-neuronal signals at time *t* of M regions, A is an $M \times M$ connection matrix wherein C_j is an $M \times M$ connection matrix ensued by modulatory input $v_j(t)$, *J* is the number of modulatory inputs. The non-diagonal elements of C_j represent the coupling of brain regions in the presence of modulatory input $v_j(t)$. $C_j(m,n)$ denotes the strength of causal connection from n-th region to m-th region for j-th type stimulus. Therefore, latent signals ***s(t)*** in *M* regions at time *t* is a bilinear function of modulatory inputs $v_j(t)$, corresponding to deviant or standard stimulus, and its previous state ***s(t-1)***. $\boldsymbol{w}(t)$ is an $M \times 1$ state noise vector whose distribution is assumed to be Gaussian distributed with covariance matrix *Q(* $\boldsymbol{w}(t) \sim N(0, Q)$). Additionally, state noise vector at time instances *1,2,….,T (* $\boldsymbol{w}(1), \boldsymbol{w}(2) \ldots \boldsymbol{w}(T)$) are assumed to be identical and independently distributed (iid). Equation (1) represents the time evolution of latent signals in M brain regions. More specifically, the latent signals at time *t*, $\boldsymbol{s}(t)$, is expressed as a linear combination of latent signals at time *t-1*, external stimulus at time t ($u(t)$), bilinear combination of modulatory inputs $v_j(t)$, $j = 1,2..J$ and its

previous state, and state noise $\boldsymbol{w}(t)$. The latent dynamics modeled in Equation (1) gives rise to observed fMRI time series represented by Equations (2) and (3).

We model the fMRI time series in region *"m"* as a linear convolution of hemodynamic response function (HRF) and latent signal $\boldsymbol{s}_m(t)$ in that region. To represent this linear convolution model as an inner product of two vectors, the past *L* values of $\boldsymbol{s}_m(t)$ are stored as a vector. $\boldsymbol{x}_m(t)$ in equation (2) represents an $L \times 1$ vector with L past values of latent signal at m-th region.
In Equation (3), $y_m(t)$ is the observed BOLD signal at *t* of *m*-th region. Φ is a $p \times L$ matrix whose rows contain bases for HRF. b_m is a $1 \times p$ coefficient vector representing the weights for each basis function in explaining the observed BOLD signal $y_m(t)$. Therefore, the HRF in *m-th* region is represented by the product $b_m\Phi$. The BOLD response in this region is obtained by convolving HRF $(b_m\Phi)$ with the *L* past values of the region's latent signal $(\boldsymbol{x}_m(t))$ and is represented mathematically by the vector inner product $b_m\Phi\, \boldsymbol{x}_m(t)$. Uncorrelated observation noise $\boldsymbol{e}_m(t)$ with zero mean and variance σ_m^2 is then added to generate the observed signal $y_m(t)$. $\boldsymbol{e}_m(t)$ is also assumed to be uncorrelated with $\boldsymbol{w}(\tau)$, at all *t* and τ. Equation (3) represents the linear convolution between the embedded latent signal $\boldsymbol{x}_m(t)$ and the basis vectors for HRF. Here, we use the canonical HRF and its time derivative as bases, as is common in most fMRI studies.

Equations (1-3) together represent a state-space model for estimating the causal interactions in latent signals based on observed multivariate fMRI time series. Furthermore, MDSI model also takes into account variations in HRF as well as the influences of modulatory and external stimuli in estimating causal interactions between the brain regions.

Estimating causal interactions between *M* regions specified in the model is equivalent to estimating the parameters $C_j, j = 1,2..J$. In order to estimate C_j's, the other unknown parameters Q, $\{b_m\}_{m=1}^{M}$ and $\{\sigma_m^2\}_{m=1}^{M}$ and the latent signal $\{\boldsymbol{s}(t)\}_{t=1}^{T}$ based on the observations $\{y_m^s(t)\}_{m=1,s=1}^{M,S}, t = 1,2..T$, where *T* is the total number of time samples and *S* is number of subjects, needs to be estimated. We use a variational Bayes approach (VB) for estimating the posterior probabilities of the unknown parameters of the MDSI model given fMRI time series observations for *S* number of subjects. The statistical significance of the parameters is assessed by examining the posterior probabilities of the parameters $C_j, j = 1,2..J$ at a given level of significance.

MDSI-load, -group, and –medication analysis

The significance of task-specific dynamic causal interactions in each edge was tested using simple t-test in each task condition. The significance of load effects was tested using paired t-test. Group differences between HC and PD-OFF were examined using two sample t-tests whereas the effects of dopaminergic medication in PD were examined using paired t-tests comparing PD-OFF and PD-ON. All tests were corrected for multiple comparisons using FDR correction at $p<0.05$.

MDSI-behaviour analysis

The brain-behavior relationship analysis was focused on the edges that showed significant or marginally significant load effects and group difference (e.g. rMFG→ rPPC in HL vs. LL and DL vs. LL in HC and PD-OFF groups). Pearson's correlations were examined to determine the

relation between the weights of causal interactions in rMFG→ rPPC in HL vs. LL and DL vs. LL and RT differences in the same task condition contrasts. Multiple linear regression analyses with covariates of age, sex, and mean framewise displacement, were used to estimate impact of potential confounds in MDSI-behavior analyses in each group. The statistical significance of difference in correlation coefficients between HC and PD-OFF was tested using *Fisher*'s z test and the statistical significance of difference in correlation coefficients between PD-OFF and PD-ON was tested using *Dunn* and *Clark*'s z test, and both were implemented in R package "cocor" [28].

gPPI analysis

We used generalized psychophysiological interaction (gPPI) [29, 30] to estimate non-causal task modulated connectivity between predefined ROIs. The gPPI model consisted of a physiological term, psychological terms, and PPI terms. The physiological term is the time series of the seed ROI; the psychological terms are HRF convolved main task effects of interest; and PPI terms are deconvolved raw time series of the seed ROI multiplied by main effect of interest followed by convolution with HRF. Thus, in each scan run, regressors consisted of the 1 physiological term (the seed ROI), 3 psychological terms (main task effect for LL, HL and DL), 3 PPI terms, and 6 head motion parameters. We conducted multiple gPPI analyses and, in each analysis, one of the thirteen ROIs was used as a seed and the rest were used as targets. PPI terms in each pair of seed-target ROIs on LL, HL and DL were extracted for further analyses.

Power analysis

We performed a power analysis based on cognitive-load dependent fMRI activations the Sternberg WM task [31]. We first calculated ROI activation levels in the DLPFC and striatum during the Sternberg task. In the DLPFC, 10 PD patients had a mean *t*-score of 2.10(SD 1.37) and 10 controls had a mean *t*-score of -0.12 (SD 1.23), yielding a Cohen's *d* value of 1.7. In the striatum, the 10 PD patients a mean *t*-score of 1.22 (SD 1.21) and the 10 controls had a mean *t*-score of 0.26 (SD 1.70) yielding a Cohen's *d* of 0.65. Comparing all PD patients and controls, using the more moderate Cohen's *d* value of 0.65, if we set alpha at $p = 0.05$ our sample size of 50 PD and 25 controls will provide power in the 75-85% range to detect such a difference.

Supplementary Results

Medication effects on behavioral performance

We used multiple linear regression analysis to examine whether medication factors, such as use of levodopa, use of other dopamine (DA) agonists, and levodopa equivalent daily dose (LEDD) (**Supplementary Table 1**), may confound the main effect of medication state on behavioral performance. There was no significant main effect of medication state for Accuracy (p=0.10) or RT (p=0.18) in the Sternberg task after controlling the other medication factors. In addition, we examined the relationship between LEDD and behavioral performance and found that LEDD was significantly correlated with RT in the LL condition (r=-0.34, p=0.04) but not with any other variables.

Lateralization of MFG→PPC causal link during working memory

First, we examined lateralization effect and its interaction with group. We conducted ANOVA on the HL vs. LL load effect on the MFG→PPC causal weight with a between-subject factor "group" (CTL vs. PDOFF) and a within-subject factor "hemisphere" (Right vs. Left). We found a significant interaction between group and hemisphere ($F_{1,78}$=11.58, p=0.001), a significant main effect of group ($F_{1,78}$=4.1, p<0.05), and a marginally significant main effect of hemisphere ($F_{1,78}$=2.9, p=0.09). Post-hoc analysis revealed that the load effect on MFG→PPC causal weights was significantly different between right and left hemisphere in HC (t_{43}=3.45, p=0.001) but not in PDOFF (t_{35}=1.42, p=0.16). We also conducted ANOVA on the DL vs. LL load effect on the MFG→PPC causal weight with a between-subject factor "group" (CTL vs. PDOFF) and a within-subject factor "hemisphere" (Right vs. Left). We found a significant interaction between group and hemisphere factors ($F_{1,78}$=10.32, p=0.002) and a significant main effect of hemisphere ($F_{1,78}$=4.1, p<0.05), but no significant main effect of group ($F_{1,78}$=1.4, p=0.2). Post-hoc analysis found that the load effect on MFG→PPC causal weights was significantly different

between right and left hemisphere in HC (t_{43}=3.91, p=0.0003) but not in PDOFF (t_{35}=0.95, p=0.35). Together, our finding suggests that the lateralization effect of the MFG→PPC causal link was significantly different between HC and PD-OFF.

Then, we examined lateralization effect in PD participants and its interaction with medication statues. We conducted ANOVA on the HL vs. LL load effect on the MFG→PPC causal weight with a within-subject factor "medication" (PDON vs. PDOFF) and a within-subject factor "hemisphere" (Right vs. Left). We found a significant interaction between medication and hemisphere factors ($F_{1,35}$=4.8, p=0.04) but no significant main effect of medication ($F_{1,35}$=0.1, p=0.7), and no significant main effect of hemisphere ($F_{1,35}$=0.002, p=0.96). Post-hoc analysis did not reveal that the load effect on MFG→PPC causal weights was significantly different between right and left hemisphere in PDOFF (t_{35}=1.42, p=0.16) and in PDON (t_{35}=1.99, p=0.054). We also conducted ANOVA on the DL vs. LL load effect on the MFG→PPC causal weight with a between-subject factor medication (PDON vs. PDOFF) and a within-subject factor hemisphere (Right vs. Left). We found no significant interaction between group and hemisphere factors ($F_{1,35}$=1.2, p=0.3), no significant main effect of medication ($F_{1,35}$=0.05, p=0.8) and no significant main effect of hemisphere ($F_{1,35}$=0.08, p=0.8). Post-hoc analysis did not find that the load effect on MFG→PPC causal weights was significantly different between right and left hemisphere in PDOFF (t_{35}=0.95, p=0.35) and in PDON (t_{35}=0.66, p=0.51).

Together, these results suggest that there is a significant right lateralized load effect on the MFG→PPC causal weight in HCs and this lateralization effect is greater in HCs than in PD participants.

Effects of medication order

In order to examine whether medication state order (ON then OFF versus OFF then ON) confounds medication effects on behavioral and brain measures, we included the ON versus OFF order as an independent variable and conducted linear mixed effect analyses. We also included sex as a potential confound in the analysis. In sum, we did not find that ON versus OFF order changed statistical significance of medication effect.

Dopaminergic medication does not change overall working memory performance in PD

We conducted linear mixed effect analysis with independent variables: medication (OFF, ON), order (OFF first, ON first) and sex (Female, Male), and dependent variables: ACC and RT per load condition. There was no significant effect of medication, order and sex factors on ACC and RT on any load condition (*ps*>0.05). Then we examined the effect of medication and order on load-modulation of ACC and RT (HL and DL relative to LL) and found no significant effect of medication, order and sex factors (*ps*>0.05).

Dopaminergic medication improves network-level causal interactions in PD

We conducted linear mixed effect analysis with independent variables: medication (OFF, ON), task condition (LL, HL and DL), order (OFF first, ON first) and sex (Female, Male), and dependent variables: MDSI-distance. The factor medication had a significant effect on MDSI-distance (*t*=-4.34, *p*=2.44e-05), but the factors task, order and sex did not (all *ps*>0.1).

Dopaminergic medication does not change frontoparietal causal link strength in PD

We conducted linear mixed effect analysis with independent variables: medication (OFF, ON) and order (OFF first, ON first), and dependent variables: load-modulation of rMFG→rPPC (HL,

DL relative to LL). For HL versus LL, there was not significant medication and sex effect (p>0.05) but there was significant order effect (t=3.2, p=0.002). For DL versus LL, there was not significant medication, order and sex effects (ps>0.1).

Dopaminergic modulation of the relation between rMFG→ rPPC *and behavioral performance in PD*

To examine whether medication ON versus OFF order influences the relation between rMFG→ rPPC and behavioral performance in PD, we conducted multiple linear regression analyses. Here we used the number of days between ON versus OFF session (Gap) as a linear variable in the regression model, rather than the categorical ON first versus OFF first variable. We specifically focused on the DL versus LL load modulation condition, which is the core finding in the main text. The independent variables were load modulation (DL versus LL) of rMFG→ rPPC and Gap, and the dependent variable was load modulation (DL versus LL) of RT. There were no significant effect of load modulation of rMFG→ rPPC and Gap in PDOFF (ps>0.4). However, there were significant effect of load modulation of rMFG→ rPPC in PDON (t=2.94, p=0.0006) but no significant effect of Gap (p>0.4).

Specificity of causal mechanisms: MDSI vs gPPI

In order to examine whether the main findings in the current study are specific to causal interactions between regions, we examined non-causal interactions between the same brain regions using gPPI. We first conducted a two-way ANOVA on gPPI distance with factors medication state (OFF, ON) and task condition (LL, HL and DL). There was no significant interaction between medication state and task condition ($F_{(2,70)}$ = 0.90, p = 0.39, *Cohen's f* =

0.17), no significant main effect of task condition ($F_{(2,70)}$ = 1.12, p = 0.30, *Cohen's f* = 0.18), and no significant main effect of medication state ($F_{(1,70)}$ = 0.95, p = 0.39, *Cohen's f* = 0.16). Next, we examined whether changes in network-level non-causal signaling are related to individual differences in cognitive function with dopaminergic medication. We trained a support vector regression model based on gPPI network distance between the PD-ON and PD-OFF states to predict changes in SDMT scores between ON and OFF dopaminergic medication and evaluated performance of the model using leave-one-out cross validation. Network distance changes did not predict SDMT changes between ON and OFF states (r=0.06, p=0.72). Importantly, we examined whether MDSI-based prediction is significantly greater than gPPI-based prediction. *Pearson* and *Filon's z* test showed that MDSI-based prediction is marginally better than gPPI-based prediction (z=1.57, p=0.05).

Finally, we determined whether the relation between the strength of the causal link rMFG→ rPPC and behavioral performance could be uncovered by gPPI. We found no significant relations between load-dependent modulation of the causal link rMFG→ rPPC and load effect in RT (ps>0.3). Then, we examined whether correlations between MDSI weight of the rMFG→ rPPC and Sternberg performance is significantly greater than the correlation between gPPI weight of the rMFG-rPPC and Sternberg performance. *Pearson* and *Filon's z* test show that correlations between load-dependent (LL vs. DL) MDSI weights of the rMFG-rPPC and load-dependent Sternberg RT are significantly stronger than correlations between load-dependent gPPI weights of the rMFG-rPPC and load-dependent Sternberg RT in PD-ON (z=1.67, p=0.04), but not in HC (z=0.93, p=0.17) or PD-OFF (z=0.84, p=0.20).

In sum, our findings suggest that MDSI weights are better predictors of behavioral performance than gPPI weights for PD-ON, although there was no significant difference for HC or PD-OFF.

Network analysis without cortical-STN connections in MDS results

To determine whether the main findings depended on whether the STN was included in the network model, we performed additional statistical analyses after excluding dynamic interaction between STN and other cortical and subcortical regions. First, we conducted a two-way ANOVA on MDSI-derived causal weights with factors medication state (OFF, ON) and task condition (LL, HL and DL). Although there was no significant interaction between medication state and task condition ($F_{(2,70)}$ = 0.10, p = 0.90, *Cohen's f* = 0.05) and no significant main effect of task condition ($F_{(2,70)}$ = 0.003, p = 0.99, *Cohen's f* = 0.02), there was a significant main effect of medication state ($F_{(1,70)}$ = 9.07, p = 0.005, *Cohen's f* = 0.51). Post-hoc analysis revealed that distance between PD-OFF and HC was significantly greater than that between PD-ON and HC in LL ($t_{(35)}$ = 2.10, p = 0.04, *Cohen's d* = 0.35) and HL ($t_{(35)}$ = 2.34, p = 0.02, *Cohen's d* = 0.39), and marginally significant in DL ($t_{(35)}$ = 2.02, p = 0.05, *Cohen's d* = 0.34) conditions (**Supplementary Figure S4**). These results replicate the main finding that dopaminergic medication improves network-level causal interactions in the PD group.

Next, we examined whether changes in network-level causal signaling are related to individual differences in cognitive function with dopaminergic medication. We trained a support vector regression model based on network distance between the PD-ON and PD-OFF states to predict changes in SDMT scores between ON and OFF dopaminergic medication and evaluated performance of the model using leave-one-out cross validation. Network distance changes

accurately predicted SDMT changes between ON and OFF states (r=0.33, p=0.05, **Supplementary Figure S5**). These results replicate the main findings that changes in causal signaling patterns within cognitive control circuitry contributes to cognitive changes in PD.

Table S1. Parkinson's disease (PD) patient medication information.

Medication Information	
n (%) on levodopa	33 (91.67%)
n (%) on dopaminergic (DA) agonists	10 (27.8%)
n (%) on both levodopa and DA agonists	8 (22.2%)
n (%) on amantadine	9 (25.0%)
n (%) on cholinesterase inhibitors	1 (2.8%)
Mean (SD) LEDD	580.1 (315.7)

LEDD: levodopa equivalent daily dosage

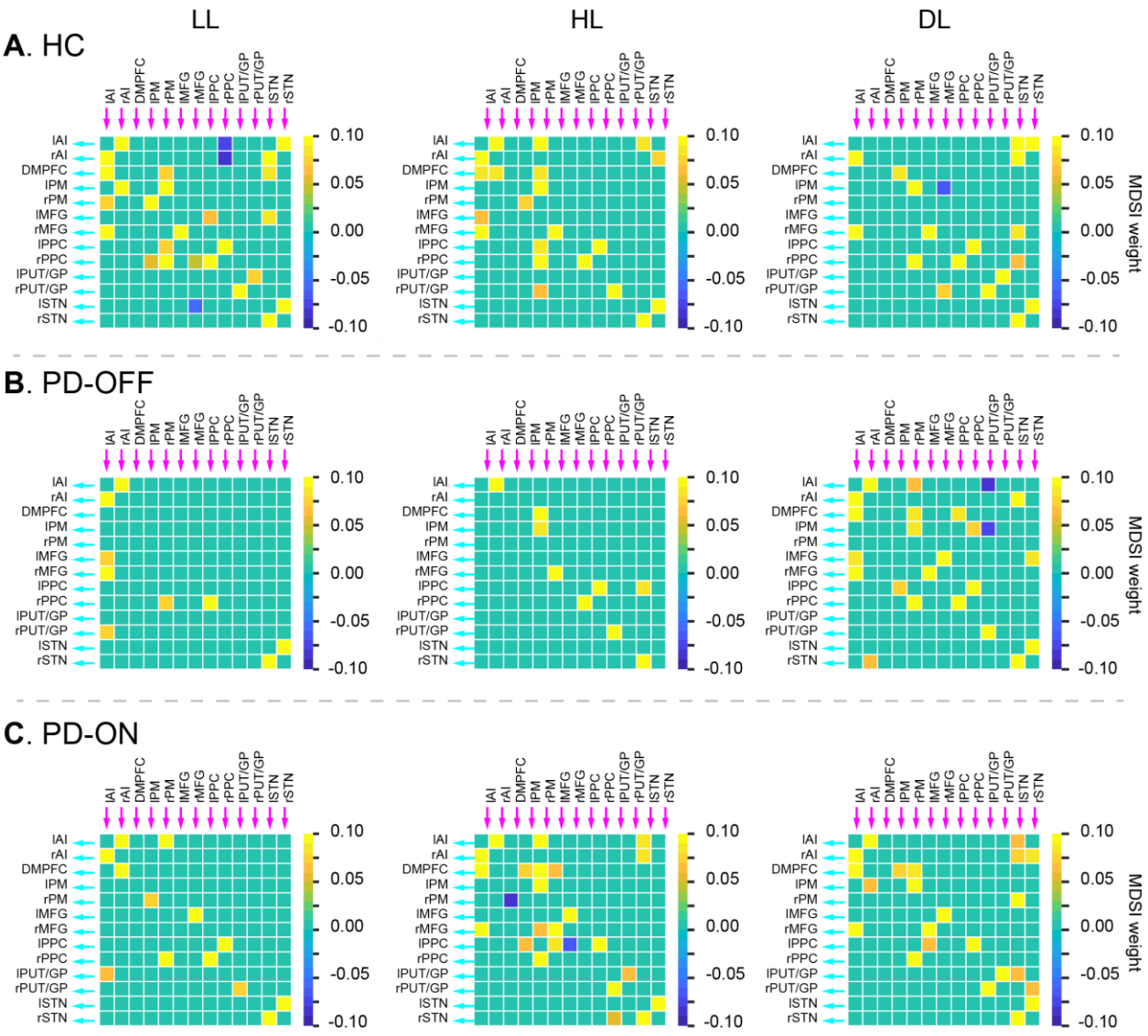

Figure S1. MDSI identified significant causal interactions between regions in the frontoparietal-basal ganglia systems in LL, HL and DL conditions in (**A**) HC, (**B**) PD-OFF and (**C**) PD-ON groups ($p < 0.05$, FDR corrected). Yellow cells indicate significant positive causal interactions and blue cells indicate significant negative causal interactions. AI: anterior insula; DMPFC: dorsomedial prefrontal cortex; PM: premotor cortex; MFG: middle frontal gyrus; PPC: posterior parietal cortex; PUT/GP = putamen/globus pallidus ; STN: subthalamic nuclei.

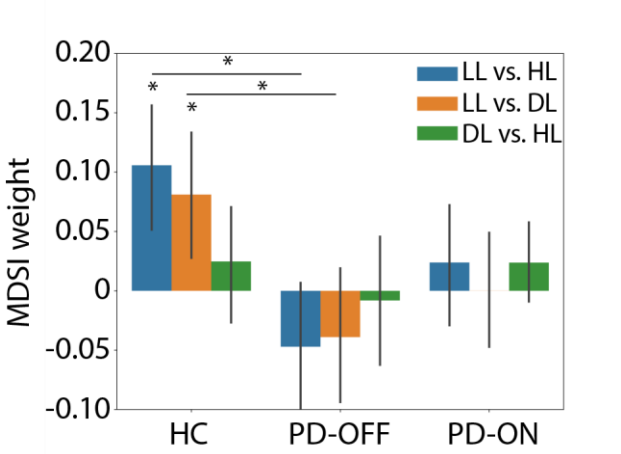

Figure S2. The strength of causal interactions from the right middle frontal gyrus to right posterior parietal cortex (rMFG→rPPC) was significantly lower in PD-OFF group compared to healthy controls (HC). *, $p<0.05$, FDR corrected.

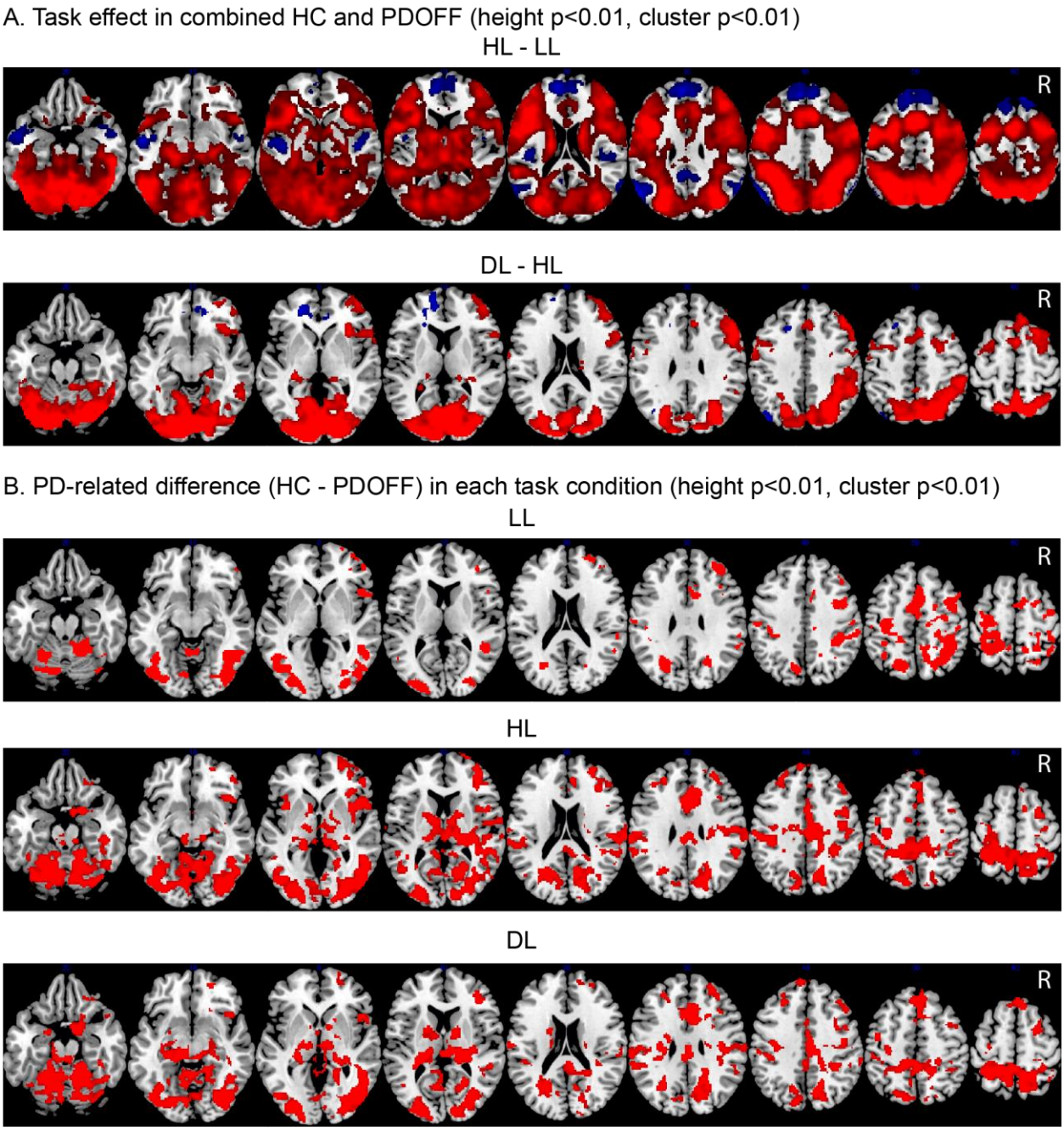

Figure S3. Activation maps from the General Linear Model: **(A)** Task effect (HL vs. LL and DL vs. HL) in combined HC and PD-OFF. **(B)** PD-related difference (HC vs. PD-OFF) in each task condition (LL, HL and DL). All maps were thresholded at height $p<0.01$ and cluster size $p<0.01$. R, right hemisphere.

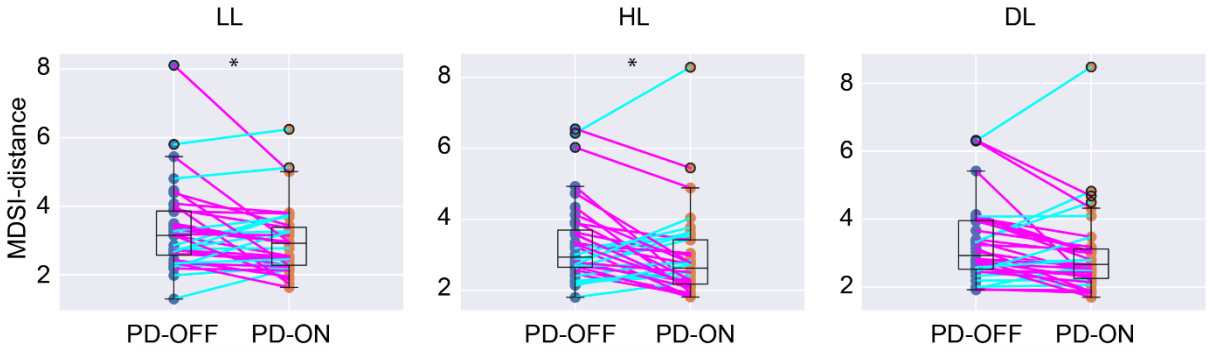

Figure S4. Dopaminergic medication reduces MDSI-based distance, which quantifies the dissimilarity in network-level causal signaling between each PD participant and the HC group, in each task condition (i.e., LL, HL, DL) (LL: $p < 0.05$, HL: $p < 0.05$, DL: $p = 0.05$). Cortical-STN connections were excluded in determining MDSI distance. *, $p<0.05$.

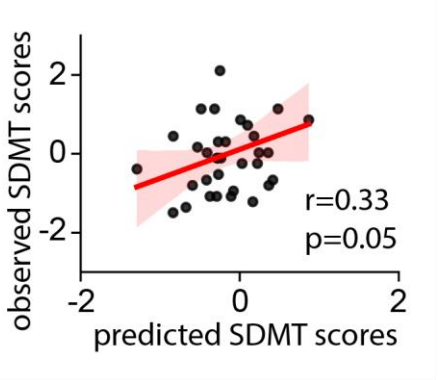

Figure S5. MDSI-based distance in causal signaling predicted change in SDMT scores between ON and OFF medication states in PD participants (r=0.33, p=0.05). Cortical-STN connections were excluded when determining MDSI distance.

Reference

1. Ashburner J. A fast diffeomorphic image registration algorithm. *Neuroimage*. Oct 15 2007;38(1):95-113. doi:10.1016/j.neuroimage.2007.07.007

2. Cai WD, Ryali S, Pasumarthy R, Talasila V, Menon V. Dynamic causal brain circuits during working memory and their functional controllability. *Nat Commun*. Jun 29 2021;12(1)doi:ARTN 3314 10.1038/s41467-021-23509-x

3. Nee DE, Brown JW, Askren MK, et al. A meta-analysis of executive components of working memory. *Cereb Cortex*. Feb 2013;23(2):264-82. doi:10.1093/cercor/bhs007

4. Owen AM, McMillan KM, Laird AR, Bullmore E. N-back working memory paradigm: a meta-analysis of normative functional neuroimaging studies. *Hum Brain Mapp*. May 2005;25(1):46-59. doi:10.1002/hbm.20131

5. Rottschy C, Langner R, Dogan I, et al. Modelling neural correlates of working memory: a coordinate-based meta-analysis. *Neuroimage*. Mar 2012;60(1):830-46. doi:10.1016/j.neuroimage.2011.11.050

6. Fan L, Li H, Zhuo J, et al. The Human Brainnetome Atlas: A New Brain Atlas Based on Connectional Architecture. *Cereb Cortex*. Aug 2016;26(8):3508-26. doi:10.1093/cercor/bhw157

7. Cavanagh JF, Wiecki TV, Cohen MX, et al. Subthalamic nucleus stimulation reverses mediofrontal influence over decision threshold. *Nat Neurosci*. Nov 2011;14(11):1462-U140. doi:10.1038/nn.2925

8. Drummond NM, Chen R. Deep brain stimulation and recordings: Insights into the contributions of subthalamic nucleus in cognition. *Neuroimage*. Nov 15 2020;222doi:ARTN 117300

10.1016/j.neuroimage.2020.117300

9. Kelley R, Flouty O, Emmons EB, et al. A human prefrontal-subthalamic circuit for cognitive control. *Brain*. Jan 1 2018;141(1):205-216. doi:10.1093/brain/awx300

10. Weintraub DB, Zaghloul KA. The role of the subthalamic nucleus in cognition. *Rev Neurosci*. 2013;24(2):125-38. doi:10.1515/revneuro-2012-0075

11. Kleiner-Fisman G, Herzog J, Fisman DN, et al. Subthalamic nucleus deep brain stimulation: summary and meta-analysis of outcomes. *Mov Disord*. Jun 2006;21 Suppl 14:S290-304. doi:10.1002/mds.20962

12. Lozano AM, Lipsman N, Bergman H, et al. Deep brain stimulation: current challenges and future directions. *Nat Rev Neurol*. Mar 2019;15(3):148-160. doi:10.1038/s41582-018-0128-2

13. Eagle DM, Baunez C, Hutcheson DM, Lehmann O, Shah AP, Robbins TW. Stop-signal reaction-time task performance: role of prefrontal cortex and subthalamic nucleus. *Cereb Cortex*. Jan 2008;18(1):178-88. doi:10.1093/cercor/bhm044

14. Fife KH, Gutierrez-Reed NA, Zell V, et al. Causal role for the subthalamic nucleus in interrupting behavior. *Elife*. Jul 25 2017;6doi:10.7554/eLife.27689

15. Pasquereau B, Turner RS. A selective role for ventromedial subthalamic nucleus in inhibitory control. *Elife*. Dec 4 2017;6doi:10.7554/eLife.31627

16. Schmidt R, Leventhal DK, Mallet N, Chen FJ, Berke JD. Canceling actions involves a race between basal ganglia pathways. *Nat Neurosci*. Aug 2013;16(8):1118-U194. doi:10.1038/nn.3456

17. Aron AR, Poldrack RA. Cortical and subcortical contributions to Stop signal response inhibition: role of the subthalamic nucleus. *J Neurosci*. Mar 1 2006;26(9):2424-33. doi:10.1523/JNEUROSCI.4682-05.2006

18. Cai W, Duberg K, Padmanabhan A, et al. Hyperdirect insula-basal-ganglia pathway and adult-like maturity of global brain responses predict inhibitory control in children. *Nat Commun*. Oct 22 2019;10(1):4798. doi:10.1038/s41467-019-12756-8

19. Swann N, Poizner H, Houser M, et al. Deep brain stimulation of the subthalamic nucleus alters the cortical profile of response inhibition in the beta frequency band: a scalp EEG study in Parkinson's disease. *J Neurosci*. Apr 13 2011;31(15):5721-9. doi:10.1523/JNEUROSCI.6135-10.2011

20. van den Wildenberg WPM, van Boxtel GJM, van der Molen MW, Bosch DA, Speelman JD, Brunia CHM. Stimulation of the subthalamic region facilitates the selection and inhibition of motor responses in Parkinson's disease. *J Cognitive Neurosci*. Apr 2006;18(4):626-636. doi:DOI 10.1162/jocn.2006.18.4.626

21. Forstmann BU, Keuken MC, Jahfari S, et al. Cortico-subthalamic white matter tract strength predicts interindividual efficacy in stopping a motor response. *Neuroimage*. Mar 2012;60(1):370-375. doi:10.1016/j.neuroimage.2011.12.044

22. Ryali S, Chen TW, Supekar K, et al. Multivariate dynamical systems-based estimation of causal brain interactions in fMRI: Group-level validation using benchmark data, neurophysiological models and human connectome project data. *J Neurosci Meth*. Aug 1 2016;268:142-153. doi:10.1016/j.jneumeth.2016.03.010

23. Ryali S, Shih YYI, Chen TW, et al. Combining optogenetic stimulation and fMRI to validate a multivariate dynamical systems model for estimating causal brain interactions. *Neuroimage*. May 15 2016;132:398-405. doi:10.1016/j.neuroimage.2016.02.067

24. Ryali S, Supekar K, Chen T, Menon V. Multivariate dynamical systems models for estimating causal interactions in fMRI. *Neuroimage*. Jan 15 2011;54(2):807-23.

25. Cai W, Chen T, Ryali S, Kochalka J, Li CSR, Menon V. Causal Interactions Within a Frontal-Cingulate-Parietal Network During Cognitive Control: Convergent Evidence from a Multisite-Multitask Investigation. *Cereb Cortex*. May 2016;26(5):2140-2153. doi:10.1093/cercor/bhv046

26. Chen T, Michels L, Supekar K, Kochalka J, Ryali S, Menon V. Role of the anterior insular cortex in integrative causal signaling during multisensory auditory-visual attention. *Eur J Neurosci*. Jan 2015;41(2):264-74. doi:10.1111/ejn.12764

27. Supekar K, Menon V. Developmental maturation of dynamic causal control signals in higher-order cognition: a neurocognitive network model. *PLoS Comput Biol*. Feb 2012;8(2):e1002374. doi:10.1371/journal.pcbi.1002374

28. Diedenhofen B, Musch J. cocor: A Comprehensive Solution for the Statistical Comparison of Correlations. *Plos One*. Apr 2 2015;10(4)doi:ARTN e0121945 10.1371/journal.pone.0121945

29. Friston KJ, Buechel C, Fink GR, Morris J, Rolls E, Dolan RJ. Psychophysiological and modulatory interactions in neuroimaging. *Neuroimage*. Oct 1997;6(3):218-29. doi:10.1006/nimg.1997.0291

30. McLaren DG, Ries ML, Xu G, Johnson SC. A generalized form of context-dependent psychophysiological interactions (gPPI): a comparison to standard approaches. *Neuroimage*. Jul 16 2012;61(4):1277-86. doi:10.1016/j.neuroimage.2012.03.068

31. Poston KL, YorkWilliams S, Zhang K, et al. Compensatory Neural Mechanisms in Cognitively Unimpaired Parkinson Disease. *Ann Neurol*. Mar 2016;79(3):448-463. doi:10.1002/ana.24585

32. Dockes J, Poldrack RA, Primet R, et al. NeuroQuery, comprehensive meta-analysis of human brain mapping. *Elife*. Mar 4 2020;9doi:10.7554/eLife.53385